New particle formation events can reduce cloud droplets in boundary layer clouds at the continental scale

D. Patoulias[1], K. Florou[1], S. N. Pandis[1,2*] and A. Nenes[1,3*]

[1]Institute for Chemical Engineering Sciences, Foundation for Research and Technology Hellas, Patras, GR-26504, Greece

[2]Department of Chemical Engineering, University of Patras, GR-26504, Greece

[3]School of Architecture, Civil & Environmental Engineering, Ecole polytechnique fédérale de Lausanne, CH-1015, Lausanne, Switzerland

Corresponding author: Athanasios Nenes, Spyros Pandis
Email: athanasios.nenes@epfl.ch; spyros@chemeng.upatras.gr

Key Points

- New particle formation (NPF) events have always been thought to increase the concentration of particles that form cloud droplets thus always lead to climate cooling
- Through high resolution modeling it is showed that stratiform clouds influenced by NPF events may experience systematic reductions in droplet leading to local warming from reductions in cloud albedo, while droplet number is always enhanced in convective clouds
- These effects combined could bear important impacts on cloud properties and structure following NPF events

Abstract

New particle formation (NPF) substantially contributes to global cloud condensation nuclei (CCN), and their climate impacts. Individual NPF events are also thought to increase local CCN, cloud droplet number (CDN), and cloud albedo. High resolution simulations however go against the latter, showing that radiatively important stratiform clouds can experience a systematic and substantial decrease in CDN during and after NPF events. CDN drops because particles too small to act as CCN uptake condensable material, and stunt the growth of particles that would otherwise form droplets. Convective clouds however experience modest increases in CDN – consistent with established views on the NPF-cloud link. Together, these results reshape our conceptual understanding of NPF impacts on clouds, as the newly discovered duality of responses would drive cloud systems in a fundamentally different manner than thought.

Plain Language Summary

Most studies assume that cloud condensation nuclei (CCN) changes directly reflect cloud droplet number (CDN) responses in clouds, ignoring the growth of pre-existing particles and their contribution to CCN. High resolution state-of-the-art simulations over Europe portray that while convective clouds experience modest increases in CDN, the radiatively important stratiform clouds may present a systematic and substantial decrease in droplet number during and after new particle

formation (NPF) events. Consequently, it is evident that NPF exhibits a duality in response – which depending on the local conditions may vitally change the manner which cloud systems may respond.

1. Introduction

Aerosols affect climate directly by scattering and absorbing solar radiation, and indirectly by affecting the number of droplets and ice crystals that form in clouds (Rosenfeld et al., 2014; Seinfeld et al., 2016). Aerosols are thought to exert a net cooling on climate, mitigating some of the warming from greenhouse gases – although with a magnitude that remains highly uncertain (Ehn et al., 2014; Kerminen et al., 2012), owing to the complexity of particle-cloud interactions across different lengthscales (Petäjä et al., 2016; Wendisch et al., 2016). New particle formation (NPF), the process by which new particles are formed directly from the gas phase, significantly affects the number concentration of particles throughout the atmosphere (Dunne et al., 2016; Kulmala et al., 2004, 2013). NPF occurs either in discrete "events", during which concentrations of nanoparticles can increase by orders of magnitude or in "non-event" days and are characterized as quiet NPF (Kulmala et al., 2022). These new particles initially are too small to affect clouds, but over time can grow enough to act as cloud condensation nuclei (CCN). Model studies indicate that over 50% of global CCN can originate from NPF (Merikanto et al., 2009; Spracklen et al., 2008; Westervelt et al., 2014) and control background levels. Field studies can also show a noticeable amplification in the number of CCN during NPF events (Sihto et al., 2011; Wiedensohler et al., 2009), as quantified by the difference in CCN concentration after and before an NPF event (Kalkavouras et al., 2019). These studies however ignore the growth of preexisting particles and their contribution to CCN during these photochemically active periods.

A majority of studies (observational or modeling) estimate the NPF impacts on clouds through its effect on CCN at prescribed supersaturation levels, or by a "CCN proxy" based on the particles exceeding a prescribed size (e.g., 100 nm diameter) (Asmi et al., 2011; Kerminen et al., 2012). This approach assumes that CCN changes directly reflect cloud droplet number responses in clouds, but it requires that water vapor supersaturation remains constant in clouds and is unaffected by CCN levels. However, this is not the case, given that supersaturation levels respond to changes in CCN levels in a way that may largely mitigate its effect on CDN (Nenes et al., 2001; Sullivan et al., 2016; Twomey, 1977). Omitting the droplet formation step in NPF-cloud interaction studies provides an incomplete – even biased - depiction of its potential impact on clouds and climate (Kalkavouras et al., 2017, 2019; Sullivan et al., 2016), as it creates the expectation that NPF events always lead to increases in CDN, hence climate cooling. For example, analysis of the aerosol-CDN link in the Eastern Mediterranean during NPF episodes over a 7-year period demonstrates a significant increase (87%) in the number of CCN, but only a modest elevation of cloud droplets (13%) for stratiform cloud conditions seen only late in the afternoon and/or early evening (Kalkavouras et al., 2017, 2019).

Understanding which atmospheric states and cloud types would respond with an increase (or decrease) in CDN during NPF events remain unclear, but fundamentally important for understanding NPF impacts on the hydrological cycle and climate. A few modeling studies, such as Sullivan et al. (2018) explicitly resolve changes in CDN due to NPF, but still uncertainties exist. The effects of growing, pre-existing particles and water vapor supersaturation changes in clouds affected by NPF needs to be considered to fully capture the impacts on CCN and CDN. Here we address this question using the state-of-the-art chemical transport model PMCAMx-UF

(Fountoukis et al., 2012; Jung et al., 2010; Patoulias and Pandis, 2022; Patoulias et al., 2018) with explicit two-moment bin microphysics to simulate the generation of new particles by nucleation, their subsequent growth, transport and their interaction with pre-existing particles. These interactions shape the CCN distributions and are coupled with a state-of-the-art droplet formation module which determines how NPF impacts CDN throughout Europe and for a variety of cloud formation conditions.

2. Methods

The cloud droplet number concentrations (CDN) and maximum supersaturation for clouds forming in the modeling domain are calculated based on the PMCAMx-UF predictions for aerosol chemical composition, size distribution, and for two cloud updraft velocities. We use the droplet parameterization based on the “population splitting” concept which later improved updrafts and largely captures the CDN that form in ambient clouds (Ghan et al., 2011; Morales Betancourt and Nenes, 2014; Morales et al., 2011; Nenes and Seinfeld, 2003). This parameterization determines the maximum supersaturation (S_{max}) developed in an ascending air parcel, and then CDNC is computed as the subset of CCN with a critical supersaturation (S_c) less than S_{max}. The maximum supersaturation is obtained when the supersaturation production, due to expansion cooling, is balanced by the water-vapor depletion from condensation.

3. Results

3.1 The effect of NPF on the total number of boundary layer cloud droplets over time

PMCAMx-UF (Information about the model features can be found in the S1) is applied over Europe for summer and spring periods for which it has been extensively evaluated (Fountoukis et al., 2012; Patoulias and Pandis, 2022; Patoulias et al., 2018) to ensure that the simulations represent a broad range of conditions during which NPF takes place. From the simulated aerosol fields, we compute the CCN concentrations and potential CDN (i.e., the droplets that are activated when clouds form) as a function of time and space, for two fixed characteristic levels of cloud-scale updraft velocity values – one that corresponds to stratiform clouds (with a vertical velocity spectral dispersion, σ_w, equal to 0.3 m s^{-1}) and one for more convective conditions (σ_w = 0.6 m s^{-1}; see SI). We then calculate the difference between simulations with and without NPF, focusing on the continental region of Europe for this analysis (Fig. S1). The CDN expresses the “potential” droplet number in clouds – as it is calculated for the cloudy fraction of every grid cell and time step regardless (as normally done in atmospheric models), and is done to fully understand the possible impacts of NPF on cloud formation (as droplet nucleation is the direct microphysical link between aerosols and clouds). Our analysis focuses on the relative change in CDN, given that it drives albedo change and other cloud impacts relevant for climate.

Fig. 1 shows results for selected days considering CDN calculated with σ_w = 0.3 m s^{-1}. The daily spatial distribution of the CDN changes is shown for two days (June 11, 25) for which the total number of potential CDN over Europe increases on average from NPF effects and a near-zero change for three more (June 16, 28, and July 8). However, the total number of potential CDN over Europe does not fully reflect the range of NPF impacts, as there are broad regions for which NPF causes a decrease in CDN, as large as 60%, even for days where NPF causes a net increase of CDN over Europe (e.g., June 11, 25). Because of this, we compute the probability distribution of droplet number change from NPF over continental Europe, and determine the fraction of the domain where droplet number decreases (by more than 5%), remains unaffected (droplet number between -5 and

5%) and increased (more than 5%) by NPF (Fig. 1f-j, k). These CDN change ranges are taken given that droplet number perturbations above 10% is when climatically-relevant changes in cloud albedo can occur. Although the net effect of NPF, continent wide, on CDN may be positive, there are considerable areas with a net decrease.

NPF average impacts on the total average CDN in the continental area range between -5 and 20% (Fig. 1k), with an average of ~ 9%. At the same time, NPF decreases CDN over 30-40% of the domain area, does not affect CDN over 10-20% of the region and leads to a net increase over the remaining 40-50% (Fig. 1l). This means that about half of the continent experiences a decrease or near-zero change in CDN after NPF events. Throughout the simulated period, CDN systematically decreased over Northern Europe, and increased for the remaining region (Fig. 2a). The maximum supersaturation, S_{max}, increases almost everywhere over continental Europe, because decreases in CDN leads to less competition of activated CCN for water vapor during the initial stages of cloud formation, which means a higher S_{max} (Fig. 2c). The S_{max} anticorrelation with CDN change (Fig. 2a, c) also means that S_{max} adjustments partially compensate for CCN changes from NPF. For the spring simulation period (April 26 to June 16, 2013) the change in total CDN concentration over Europe was also complex (Fig. S2). Decreases in CDN from NPF are predicted for a region covering approximately 30-50% of Europe (Fig. S2l).

For an updraft velocity of $\sigma_w = 0.6$ m s^{-1}, the CDN increases due to NPF almost everywhere (Fig. 2b), because the higher S_{max} generated can activate smaller particles (compared to $\sigma_w = 0.3$ m s^{-1}) which are generally increased by NPF. The fraction of total average CDN increases by 10-60% (Fig. S3k), with a domain average of 26 %. Even here, however, a CDN reduction of 10-30% is predicted in many areas (Fig. S3l). For $\sigma_w = 0.6$ m s^{-1}, the S_{max}, depending on the location may increase or decrease, or just change slightly (±5%), with the total change fluctuating between -25 and 2% (Fig. S5k).

The diameter above which aerosol activates into cloud droplets (the "activation diameter") is often assumed to be constant between 50 and 160 nm, corresponding roughly to clouds with S_{max} between 1% and 0.1%, respectively (Asmi et al., 2011). For low S_{max} (0.1%), the CCN concentration and the number of particles with diameter larger than 160 nm, N_{160}, decrease in many parts of Europe with the least change observed in Central and South Europe (Fig. 2g, f). The CDN is decreased mainly in Southern Spain and Central-Northern Europe (Fig.2a) because this is where the largest increase in the number of particles between 25 and 100 nm in diameter ($N_{25\text{-}100}$; Aitken mode particles) tends to be seen. The formation of new particles creates additional particle surface for condensation, which scavenges the mass that would otherwise be added to larger particles. At low S_{max} values (~0.1%), NPF reduces the number of large CCN, and allows supersaturation to build up more during the original stages of cloud formation (Morales Betancourt and Nenes, 2014) which causes a slight increase in S_{max} and activated CCN. In contrast, the growth of new particles removes condensable material from the gas phase, and deprives it from larger particles, resulting in a reduced number of particles that can act as CCN and reduced droplet number (Fig. S10). NPF is predicted to cause an increase in N_{100} and N_{130} in many regions but a decrease in N_{200} and N_{260} almost everywhere (Fig. S6-9). For higher supersaturation (0.2%), the number of CCN from NPF events increases everywhere, especially in South and East Europe (Fig. 2h and Fig S10).

The average simulated CCN spectra in the boundary layer with and without nucleation effects show very clearly the integrated impacts of NPF and can be used to determine the supersaturation range for which a reduction (or increase) is seen. Fig. 3 shows such results for three locations in North Europe and three in the South. At all sites, there is a reduction in CCN for the lowest supersaturations when NPF is active, so that cloud formation at such conditions would result in reductions in droplet number. At higher supersaturations, the reverse effect is seen – NPF leads to a net increase in droplet number. A characteristic "crossover" supersaturation can therefore be defined, where NPF switches from decreasing to increasing CCN (and corresponds to where the curves in Fig. 3 intersect) and droplet number. For North Europe, the crossover supersaturation ranges from 0.15-0.2%, while for South Europe it is at 0.1% or lower. This has profound impacts on how clouds respond to NPF perturbations – and also explains why there tends to be a net increase in droplet number in the simulations in the South and vice-versa.

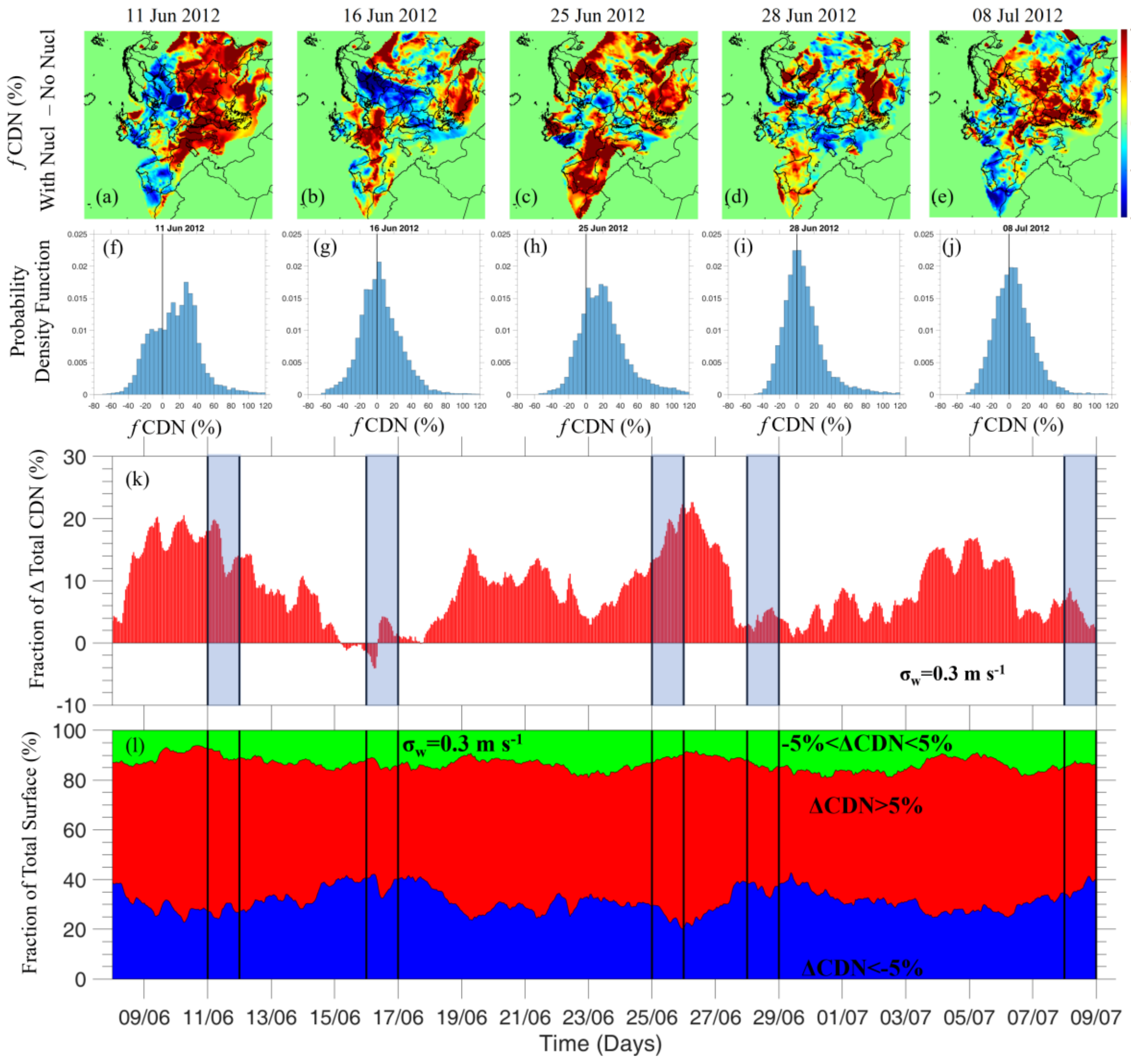

Figure 1. The maps show the daily average fractional increase change in the number of droplets due to nucleation events for updraft velocity of σ_w = 0.3 m s^{-1} for: June 11 (a), 16 (b), 25 (c), 28 (d) and July 8 (e), 2012. The probability density as a function of fractional increase change in the number of droplets due to nucleation events for June 11 (f), 16 (g), 25 (h), 28 (i) and July 8 (j), 2012 is shown. The hourly ground-level average fractional increase change in the number of cloud droplets due to nucleation for continental Europe as a function of time for the 2012 simulated period for updraft velocity of σ_w = 0.3 m s^{-1} is depicted in (k). The hourly ground-level average

fraction of surface as a function of time for the 2012, where blue is the area of the average fractional increase change in the number of droplets (ΔCND) due to nucleation less than -5%, red is for ΔCND higher than 5%, and, green is the ΔCND between -5 % and 5%.

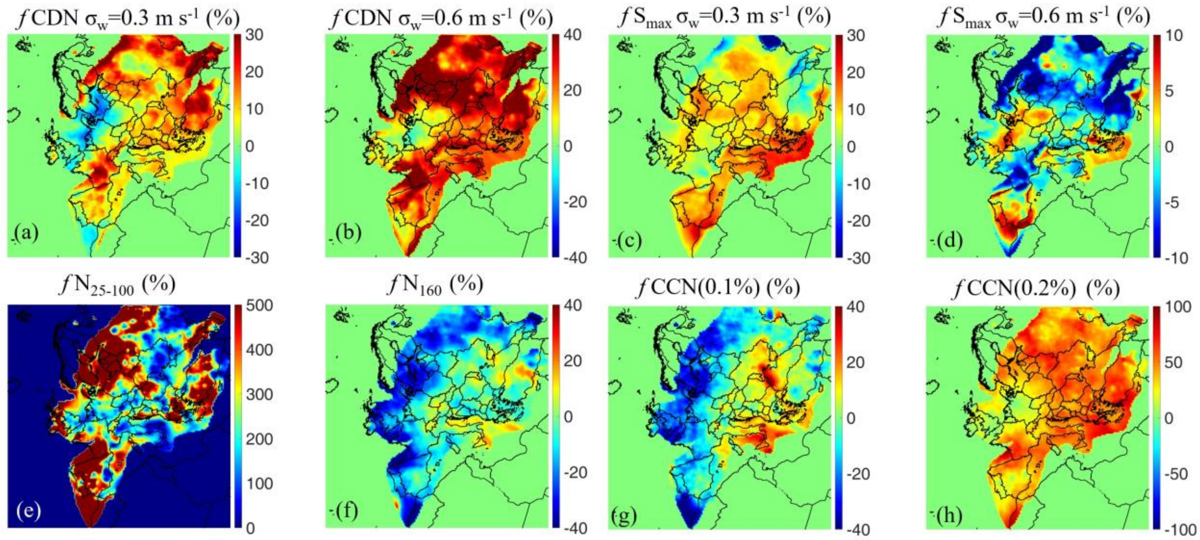

Figure 2. The ground-level predicted average fractional increase change (%) due to NPF in CDN for updraft velocity (a) σ_w = 0.3 m s^{-1} and (b) σ_w = 0.6 m s^{-1}; the maximum supersaturation of clouds for (c) σ_w = 0.3 m s^{-1} and (d) σ_w = 0.6 m s^{-1}; (e) the concentration of particles with a diameter between 25 nm and 100 nm ($N_{25\text{-}100}$) and (f) the concentration of particles with a diameter greater than 160 nm (N_{160}); the concentration of CCN at (g) 0.1% and (h) 0.2% supersaturation. Results shown are averaged over the 5 June to 8 July 2012 period.

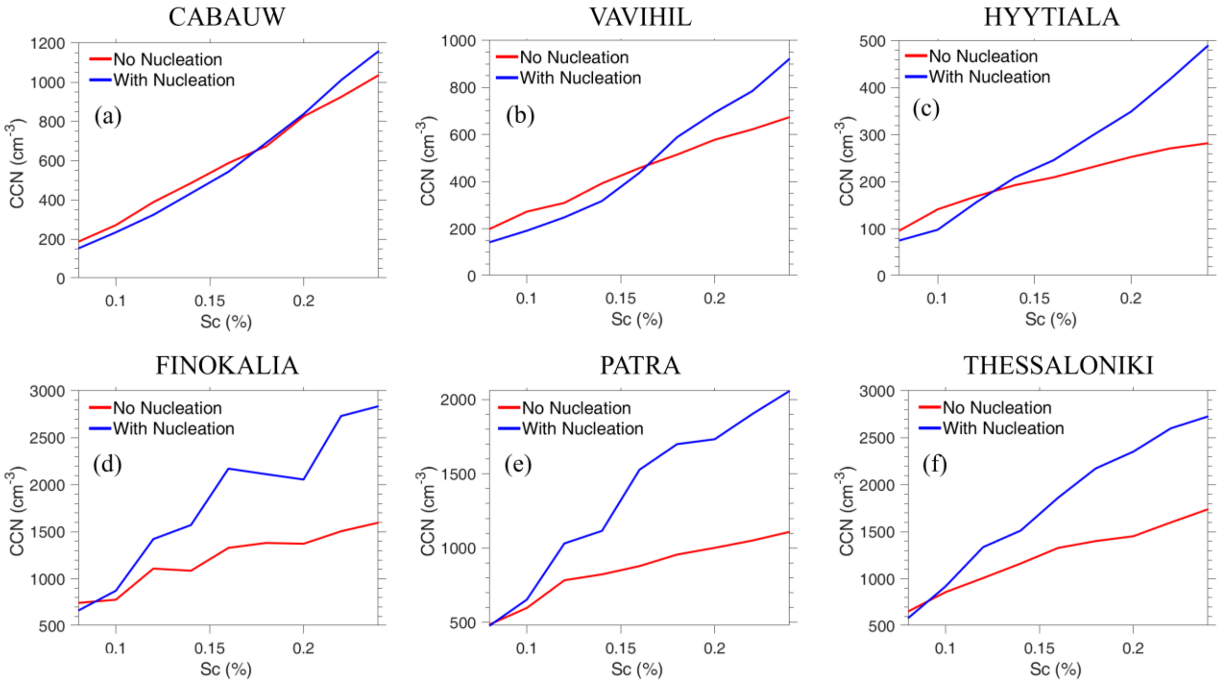

Figure 3. Average CCN spectra (cm^{-3}) function as supersaturation (%)at three North European sites (top row, Cabauw-Netherlands; Vavihill-Sweden; Hyytiala-Finland) and three Southern European sites (bottom row, Finokalia; Patra; Thessaloniki-Greece). Simulations with NPF effects are shown in blue and without NPF effects in red. Results shown are averaged over the 5 June to 8 July 2012 period.

3.2 Evolution of number distributions and effect on number of droplets

The PMCAMx-UF predictions in specific locations can be used to elucidate the NPF effect on the diurnal cycle of CDN. This is important, as the timing of CDN changes determines how much cloud radiative forcing can change (Kalkavouras et al., 2017). The results for Cabauw (Netherlands) are used as an example (Fig. S13). In the base case simulation, NPF events were predicted on 3 out of the 4 days shown and started at around 8:00 UTC. The predicted CDN for σ_w = 0.3 and 0.6 m s^{-1} is higher when NPF is inactive (Figs. S13b, S13c). The effect of NPF on the CDN is predicted to appear 2-3 h after the nucleation event, which corresponds to the afternoon and early evening hours after the peak of the solar forcing. During this time, the new particles grow to diameters more than 25 nm, and the $N_{25\text{-}100}$ concentration increases (Fig. S13g). As a result, nucleation in this case leads to N_{100} reduction (Fig. S13f). For the day without NPF (24 June 2012), the predicted concentration of droplets is almost the same for the two simulations, with a small difference present due to particles being transported from other areas where nucleation has occurred.

The temporal effect of NPF on CDN can be also analyzed in Cabauw by examining the average diurnal variation of the aerosol and droplet number concentrations (Fig. 4 and Fig. S14). In the morning hours, CDN do not substantially differ. A few hours after the NPF, the predicted CDN is reduced, compared to the simulation without NPF effects. The largest CDN difference is predicted from 13:00 to 22:00 UTC for the less turbulent boundary layer (σ_w = 0.3 m s^{-1}). During the night hours the number of droplets is not affected by the previous day's nucleation event. Regarding the more convective case, the effect is on average present until 21:00 UTC.

In Vavihill (Sweden), Cabauw (Netherlands) and Birkenes (Norway), a reduction in CDN from NPF is predicted for σ_w=0.3 ms^{-1} (Fig. S15). In Vavihill, CDN with nucleation is found to be lower for all hours with the maximum CDN reduction occurring at 7:00 UTC. At Birkenes and Cabauw, CDN effects are most prominent noon and afternoon, when cloud forcing can be quite strong. At Finokalia (Greece), K-puszta (Hungary), and Hyytiala (Finland) NPF generally increases CDN (Fig. S15a); for σ_w = 0.3 m s^{-1} the CDN enhancement is 6%, consistent with the 7-12% increase found by Kalkavouras et al. (2019) during their 7-year study found at the same location. As in Cabauw and the other sites, the increase in droplet number occurs later in the afternoon and the evening.

Throughout this study, we focused on potential CDN without considering the extent to which clouds actually form in the region affected by NPF. Although we do not carry out this analysis here, the meteorological simulations that are used to drive the PMCAMx-UF simulations clearly show that clouds systematically form in regions with negative ΔCDN (Fig. S16). Furthermore, the frequency with which CDN decreases from the effect of NPF throughout Europe (on average, 30%) means that there will always be some cloud present in regions influenced by CCN reduction from the effect of NPF. This means that the cloud albedo reduction effect is an unappreciated – yet potentially important – component of the climate forcing from NPF.

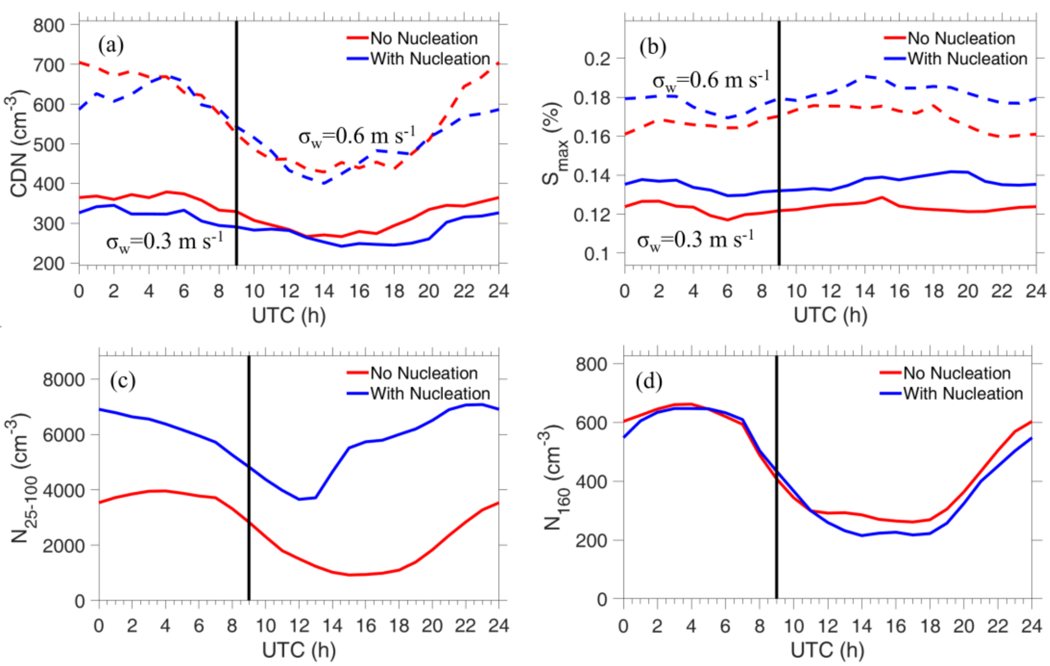

Figure 4. Daily average (5 June to 8 July 2012) profiles for Cabauw including NPF (blue lines) and without NPF (red lines) of the: (a) cloud droplet number concentration (CDN) for updraft velocity of σ_w = 0.3 m s^{-1} (straight lines) and σ_w = 0.6 m s^{-1} (dashed lines); (b) maximum cloud supersaturation (S_{max}) for updraft velocity σ_w = 0.3 m s^{-1} (straight lines) and σ_w = 0.6 m s^{-1} (dashed lines), (c) the concentration of particles of diameter between 25 nm and 100 nm (N_{25-100}) and (d) the concentration of particles of diameter greater than 160 nm (N_{160}). The black line indicates the average time where NPF starts.

4. Conclusions

We show that radiatively important stratiform clouds can experience a systematic and substantial decrease in droplet number during and after nucleation events over extensive regions throughout Europe. The drop in CDN occurs because particles present prior to the NPF experience slower growth during and after each event, leading to fewer CCN for clouds with S_{max} characteristic of stratiform clouds (~0.1-0.2%; Fig. 5). Convective clouds, however, are characterized by relatively high supersaturations and tend to experience increases in cloud droplet number – in accordance with the established views on the NPF-cloud link (Fig. 5). These changes tend to occur 2-3 hours after the initiation of the NPF event, in the afternoon or evening, and with decreases that tend to be stronger in the North.

The above results modify our conceptual understanding of NPF impacts on clouds. Droplet concentrations in stratiform clouds may be unaffected or even reduced (leading to local warming from reductions in cloud albedo) but are most frequently enhanced in convective clouds (Fig. 5). There exists a "crossover" supersaturation – below which NPF events decrease CCN and CDN – that varies but tends to be in the 0.1-0.15% range (Fig. 5). Given this, NPF events, apart from their immediate radiative effects, could bear important feedbacks on cloud structure and their temporal evolution in the vicinity of their influence. This is because cloud droplet reductions in stratiform clouds allow local warming, which subsequently may increase boundary layer turbulence, and convective activity. The importance of the above links varies considerably with location and time, but it is clear that NPF may not provide the monotonic increase in CCN and droplet number thought to date, but rather exhibit a duality in response – which depending on the local conditions may fundamentally different radiative forcing, cloud structure and precipitation.

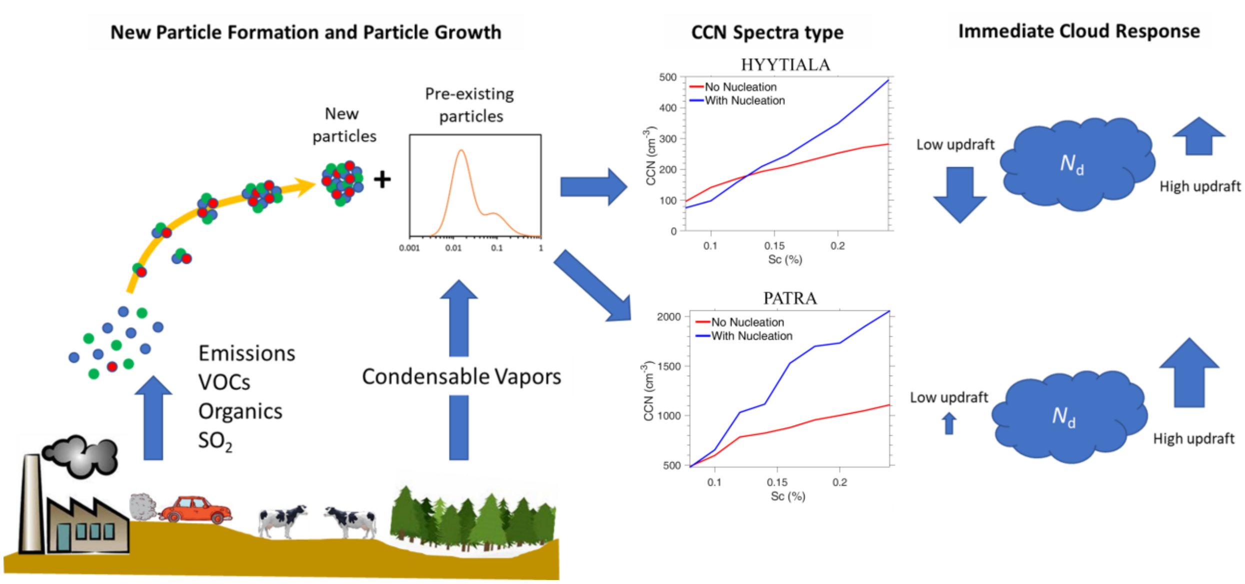

Figure 5. Sketch representing the impacts of NPF on aerosol size distribution, CCN and droplet number. Depending on the pre-existing particles, number of particles forming, available condensable vapor mass for aerosol growth and vertical velocity (i.e., cloud type), the aerosol may experience a reduction in CCN and droplet number at lower supersaturations (top graphs), or an increase in CCN and droplet number for all cloud-relevant supersaturations (bottom graphs). Blue lines indicate aerosol with the effects of NPF, and red without NPF effects.

Acknowledgments

We acknowledge support by the project PyroTRACH (ERC-2016-COG) funded from H2020-EU.1.1. - Excellent Science - European Research Council (ERC), project ID 726165 and from the European Union project FORCeS funded from Horizon H2020-EU.3.5.1 (project ID 821205).

Open Research

The data from this study are available of Envidat (https://www.doi.org/10.16904/envidat.457) and the code PMCAMx-UF is publicly accessible through the online, open-access repository of Zenodo (https://zenodo.org/doi/10.5281/zenodo.10078188).

References

Asmi, E., Kivekäs, N., Kerminen, V.-M., Komppula, M., Hyvärinen, A.-P., Hatakka, J., et al. (2011). Secondary new particle formation in Northern Finland Pallas site between the years 2000 and 2010. *Atmospheric Chemistry and Physics*, *11*(24), 12959–12972. https://doi.org/10.5194/acp-11-12959-2011

Dunne, E. M., Gordon, H., Kürten, A., Almeida, J., Duplissy, J., Williamson, C., et al. (2016). Global atmospheric particle formation from CERN CLOUD measurements. *Science*, *354*(6316), 1119–1124. https://doi.org/10.1126/science.aaf2649

Ehn, M., Thornton, J. A., Kleist, E., Sipilä, M., Junninen, H., Pullinen, I., et al. (2014). A large source of low-volatility secondary organic aerosol. *Nature*, *506*(7489), 476–479. https://doi.org/10.1038/nature13032

Fountoukis, C., Riipinen, I., Denier van der Gon, H. A. C., Charalampidis, P. E., Pilinis, C., Wiedensohler, A., et al. (2012). Simulating ultrafine particle formation in Europe using a regional CTM: contribution of primary emissions versus secondary formation to aerosol number concentrations. *Atmospheric Chemistry and Physics*, *12*(18), 8663–8677. https://doi.org/10.5194/acp-12-8663-2012

Ghan, S. J., Abdul-Razzak, H., Nenes, A., Ming, Y., Liu, X., Ovchinnikov, M., et al. (2011). Droplet nucleation: Physically-based parameterizations and comparative evaluation. *Journal of Advances in Modeling Earth Systems*, *3*(4), 1–34. https://doi.org/10.1029/2011MS000074

Jung, J., Fountoukis, C., Adams, P. J., & Pandis, S. N. (2010). Simulation of in situ ultrafine particle formation in the eastern United States using PMCAMx-UF. *Journal of Geophysical*

Research, *115*(D3), D03203. https://doi.org/10.1029/2009JD012313

Kalkavouras, P., Bossioli, E., Bezantakos, S., Bougiatioti, A., Kalivitis, N., Stavroulas, I., et al. (2017). New particle formation in the southern Aegean Sea during the Etesians: importance for CCN production and cloud droplet number. *Atmospheric Chemistry and Physics*, *17*(1), 175–192. https://doi.org/10.5194/acp-17-175-2017

Kalkavouras, P., Bougiatioti, A., Kalivitis, N., Stavroulas, I., Tombrou, M., Nenes, A., & Mihalopoulos, N. (2019). Regional new particle formation as modulators of cloud condensation nuclei and cloud droplet number in the eastern Mediterranean. *Atmospheric Chemistry and Physics*, *19*(9), 6185–6203. https://doi.org/10.5194/acp-19-6185-2019

Kerminen, V.-M., Paramonov, M., Anttila, T., Riipinen, I., Fountoukis, C., Korhonen, H., et al. (2012). Cloud condensation nuclei production associated with atmospheric nucleation: a synthesis based on existing literature and new results. *Atmospheric Chemistry and Physics*, *12*(24), 12037–12059. https://doi.org/10.5194/acp-12-12037-2012

Kulmala, M., Vehkamäki, H., Petäjä, T., Dal Maso, M., Lauri, A., Kerminen, V.-M., et al. (2004). Formation and growth rates of ultrafine atmospheric particles: a review of observations. *Journal of Aerosol Science*, *35*(2), 143–176. https://doi.org/10.1016/j.jaerosci.2003.10.003

Kulmala, Markku, Kontkanen, J., Junninen, H., Lehtipalo, K., Manninen, H. E., Nieminen, T., et al. (2013). Direct Observations of Atmospheric Aerosol Nucleation. *Science*, *339*(6122), 943–946. https://doi.org/10.1126/science.1227385

Kulmala, Markku, Junninen, H., Dada, L., Salma, I., Weidinger, T., Thén, W., et al. (2022). Quiet New Particle Formation in the Atmosphere. *Frontiers in Environmental Science*, *10*(June), 1–11. https://doi.org/10.3389/fenvs.2022.912385

Merikanto, J., Spracklen, D. V, Mann, G. W., Pickering, S. J., & Carslaw, K. S. (2009). Impact of nucleation on global CCN. *Atmospheric Chemistry and Physics*, *9*(21), 8601–8616. https://doi.org/10.5194/acp-9-8601-2009

Morales Betancourt, R., & Nenes, A. (2014). Understanding the contributions of aerosol properties and parameterization discrepancies to droplet number variability in a global climate model. *Atmospheric Chemistry and Physics*, *14*(9), 4809–4826. https://doi.org/10.5194/acp-14-4809-2014

Morales, R., Nenes, A., Jonsson, H., Flagan, R. C., & Seinfeld, J. H. (2011). Evaluation of an entraining droplet activation parameterization using in situ cloud data. *Journal of*

Geophysical Research, *116*(D15), D15205. https://doi.org/10.1029/2010JD015324

Nenes, A., & Seinfeld, J. H. (2003). Parameterization of cloud droplet formation in global climate models. *Journal of Geophysical Research*, *108*(D14), 4415. https://doi.org/10.1029/2002JD002911

Nenes, Athanasios, Ghan, S., Abdul-Razzak, H., Chuang, P. Y., & Seinfeld, J. H. (2001). Kinetic limitations on cloud droplet formation and impact on cloud albedo. *Tellus B: Chemical and Physical Meteorology*, *53*(2), 133. https://doi.org/10.3402/tellusb.v53i2.16569

Patoulias, D., & Pandis, S. N. (2022). Simulation of the effects of low-volatility organic compounds on aerosol number concentrations in Europe. *Atmospheric Chemistry and Physics*, *22*(3), 1689–1706. https://doi.org/10.5194/acp-22-1689-2022

Patoulias, David, Fountoukis, C., Riipinen, I., Asmi, A., Kulmala, M., & Pandis, S. N. (2018). Simulation of the size-composition distribution of atmospheric nanoparticles over Europe. *Atmospheric Chemistry and Physics*, *18*(18), 13639–13654. https://doi.org/10.5194/acp-18-13639-2018

Petäjä, T., O'Connor, E. J., Moisseev, D., Sinclair, V. A., Manninen, A. J., Väänänen, R., et al. (2016). BAECC: A Field Campaign to Elucidate the Impact of Biogenic Aerosols on Clouds and Climate. *Bulletin of the American Meteorological Society*, *97*(10), 1909–1928. https://doi.org/10.1175/BAMS-D-14-00199.1

Rosenfeld, D., Sherwood, S., Wood, R., & Donner, L. (2014). Climate Effects of Aerosol-Cloud Interactions. *Science*, *343*(6169), 379–380. https://doi.org/10.1126/science.1247490

Seinfeld, J. H., Bretherton, C., Carslaw, K. S., Coe, H., DeMott, P. J., Dunlea, E. J., et al. (2016). Improving our fundamental understanding of the role of aerosol−cloud interactions in the climate system. *Proceedings of the National Academy of Sciences*, *113*(21), 5781–5790. https://doi.org/10.1073/pnas.1514043113

Sihto, S.-L., Mikkilä, J., Vanhanen, J., Ehn, M., Liao, L., Lehtipalo, K., et al. (2011). Seasonal variation of CCN concentrations and aerosol activation properties in boreal forest. *Atmospheric Chemistry and Physics*, *11*(24), 13269–13285. https://doi.org/10.5194/acp-11-13269-2011

Spracklen, D. V., Carslaw, K. S., Kulmala, M., Kerminen, V.-M., Sihto, S.-L., Riipinen, I., et al. (2008). Contribution of particle formation to global cloud condensation nuclei concentrations. *Geophysical Research Letters*, *35*(6), L06808. https://doi.org/10.1029/2007GL033038

Sullivan, R. C., Crippa, P., Matsui, H., Leung, L. R., Zhao, C., Thota, A., & Pryor, S. C. (2018). New particle formation leads to cloud dimming. *Npj Climate and Atmospheric Science*, *1*(1), 9. https://doi.org/10.1038/s41612-018-0019-7

Sullivan, S. C., Lee, D., Oreopoulos, L., & Nenes, A. (2016). Role of updraft velocity in temporal variability of global cloud hydrometeor number. *Proceedings of the National Academy of Sciences*, *113*(21), 5791–5796. https://doi.org/10.1073/pnas.1514039113

Twomey, S. (1977). The Influence of Pollution on the Shortwave Albedo of Clouds. *Journal of the Atmospheric Sciences*, *34*(7), 1149–1152. https://doi.org/10.1175/1520-0469(1977)034<1149:TIOPOT>2.0.CO;2

Wendisch, M., Pöschl, U., Andreae, M. O., Machado, L. A. T., Albrecht, R., Schlager, H., et al. (2016). ACRIDICON–CHUVA Campaign: Studying Tropical Deep Convective Clouds and Precipitation over Amazonia Using the New German Research Aircraft HALO. *Bulletin of the American Meteorological Society*, *97*(10), 1885–1908. https://doi.org/10.1175/BAMS-D-14-00255.1

Westervelt, D. M., Pierce, J. R., & Adams, P. J. (2014). Analysis of feedbacks between nucleation rate, survival probability and cloud condensation nuclei formation. *Atmospheric Chemistry and Physics*, *14*(11), 5577–5597. https://doi.org/10.5194/acp-14-5577-2014

Wiedensohler, A., Cheng, Y. F., Nowak, A., Wehner, B., Achtert, P., Berghof, M., et al. (2009). Rapid aerosol particle growth and increase of cloud condensation nucleus activity by secondary aerosol formation and condensation: A case study for regional air pollution in northeastern China. *Journal of Geophysical Research*, *114*(8), D00G08. https://doi.org/10.1029/2008JD010884